Analysis of hyperspherical channels of three-electron atomic systems

Xiazhou Yang,[1] Jinhua Xi,[1,*] C. G. Bao,[2] and C. D. Lin[1]
[1]*Department of Physics, Kansas State University, Manhattan, Kansas 66506-2601*
[2]*Department of Physics, Zhong-Shan University, Guangzhou, People's Republic of China*
(Received 20 March 1995; revised manuscript received 15 May 1995)

Hyperspherical coordinates are used to study three-electron atomic systems. Within the adiabatic approximation, the Schrödinger equation for the three-electron systems is reduced to a set of partial differential equations of two hyperangles at each fixed hyper-radius. We restrict ourselves in the present paper to the configurations where the orbital angular momentum of each electron is zero. The adiabatic potential curves and the associated wave functions are obtained. We identify potential curves associated with singly, doubly, and triply excited states and analyze the nodal structure of the associated wave functions with respect to the two hyperangles.

PACS number(s): 31.10.+z, 31.15.Ja, 32.30.−r, 32.10.−f

I. INTRODUCTION

Microscopic physics is traditionally studied starting with the independent particle model where the motion of each particle is governed predominantly by the mean field of all the other particles. The early observation of doubly excited states in helium by Madden and Codling [1] in the 1960s revealed the limitation of this simple picture. In the past three decades, different new approaches [2] have been proposed which were aimed at studying doubly excited states of two-electron atoms with a departure point different from the independent electron model. One of the approaches is to employ hyperspherical coordinates [3]. Over the years, the hyperspherical approach has been used to analyze electron-electron correlation for different doubly excited states and, with the adoption of results from the algebraic approach [4], to provide a complete classification scheme for these states [5]. In recent years, the implementation of the hyperspherical close coupling method [6] illustrates that this approach is capable of performing accurate calculations for any parameters for two-electron systems such as photoionization cross sections and resonance positions and widths. The method is particularly powerful when many channels are open where other approaches are more difficult to implement.

An obvious question is whether the hyperspherical approach can be extended to many-electron systems. In atoms, when only one electron is excited, the independent electron model or the Hartree-Fock model is still mostly adequate. When two electrons are excited in a many-electron system, it is desirable to reduce the problem to an effective two-electron system which can then be treated in hyperspherical coordinates as in helium atoms [7]. On the other hand, when three or more electrons are excited, new approaches are needed. In this paper we show results of applying hyperspherical coordinates to the prototype three-electron system, Li, where the complete spectra, including singly, doubly, and triply excited states, are to be addressed at the same time.

The application of hyperspherical coordinates to n-electron systems has been addressed formally [8]. However, few actual calculations have been carried out. In their pioneer attempts, Clark and Greene calculated the hyperspherical potential curves for three-electron systems within two angular momentum configurations, s^3 [9] and s^2p [10], respectively, by using the hyperspherical harmonics as the basis functions. Another early calculation of the potential curves for He^- of $^4P^e$ symmetry was given by Watanabe, Dourneuf, and Pelamourgues [7] employing a basis of optimized Slater-type functions. These preliminary results were briefly reviewed in Ref. [11] and they showed qualitatively that the hyperspherical potential curves could be sorted into the groups supporting singly, doubly, and triply excited states, respectively. However, they were not accurate enough for a quantitative investigation. Therefore, the power and the merit of the hyperspherical approach was partially lost.

In order to achieve accurate quantitative results using the hyperspherical approach for three-electron systems, it is thus necessary to develop new numerical approaches. A direct numerical method to obtain the potential curves has been formulated recently by Bao and Lin [12] (this reference is shortened as BL hereafter). They reduced the problem to a set of partial differential equations in two hyperspherical angles which have the proper exchange symmetry for solutions with well-defined total spin and total orbital angular momentum quantum numbers, as well as parity.

In this paper we present first numerical results from the solution of the differential equations given in BL, limiting ourselves initially to the configurations where the angular momentum of each electron is zero. A brief outline of the method is presented in Sec. II, where the coordinate system and the numerical method are discussed. In Sec.

*Present address: Department of Physics, Vanderbilt University, Nashville, TN 37235.

III, the adiabatic potential curves and the singly, doubly, and triply excited states associated with these curves are discussed. The nodal structure of the associated wave function for each potential curve and the major features that distinguish singly, doubly, and triply excited states are discussed in Sec. IV. Finally, some remarks in Sec. V conclude this paper.

Triply excited states of atoms have increasingly gained attention in the past few years [13]. While some individual triply excited states have been observed over the years [14], more systematic studies from synchrotron radiation laboratories are beginning to emerge [15]. In addition to the prediction of resonance positions and widths for individual states, a classification scheme for triply excited states is desired. Such a scheme emerges only after the nature of electron correlation in three-electron systems is understood. We do not expect such a scheme to emerge immediately, but the present approach is an effort toward such a direction.

II. HYPERSPHERICAL TREATMENT FOR THREE-ELECTRON SYSTEMS

In this section, we briefly outline the hyperspherical formulation for three-electron systems. Atomic units are used throughout this paper unless explicitly stated otherwise.

The simplest hyperspherical coordinates for a three-electron atomic system is defined by replacing the radial distances of the three electrons, r_1, r_2, and r_3, by a hyperradius R and two hyperangles, α_1 and α_2,

$$\begin{aligned} r_1 &= R\sin\alpha_1\cos\alpha_2, \\ r_2 &= R\sin\alpha_1\sin\alpha_2, \\ r_3 &= R\cos\alpha_1, \end{aligned} \tag{1}$$

where $0 \le R \le \infty$ and $0 \le \alpha_1, \alpha_2 \le \pi/2$. In this coordinate system, R represents the size of the atomic system. The two angles, α_1 and α_2, measure the relative distances of the electrons from the nucleus and are used to describe the radial correlation. For the six spherical angles $\hat{r}_i$ $(i = 1, 2, 3)$, it is possible to replace them by three Euler angles which describe the rotation of the whole atom with respect to the laboratory frame and three other angles which describe the relative orientation of the electrons, or in other words, the angular correlation.

The total wave function Ψ of the three-electron system is written as

$$\Psi = \psi/(R^4 \sin^2\alpha_1 \cos\alpha_1 \sin\alpha_2 \cos\alpha_2), \tag{2}$$

where the prefactor is given by the Jacobian determinant. The volume element of α_1 and α_2 is $d(\cos\alpha_1)d\alpha_2$. The Schrödinger equation for the three-electron system can be expressed as

$$\left(-\frac{1}{2}\frac{\partial^2}{\partial R^2} + \frac{1}{2R^2}[T_s + W]\right)\psi = E\psi, \tag{3}$$

where T_s and W are given by

$$T_s = -\left(\frac{\partial^2}{\partial\alpha_1^2} + \frac{\cos\alpha_1}{\sin\alpha_1}\frac{\partial}{\partial\alpha_1} + \frac{1}{\sin^2\alpha_1}\frac{\partial^2}{\partial\alpha_2^2}\right) \tag{4}$$

and

$$W = \frac{\vec{l}_1^2}{\sin^2\alpha_1\cos^2\alpha_2} + \frac{\vec{l}_2^2}{\sin^2\alpha_1\sin^2\alpha_2} + \frac{\vec{l}_3^2}{\cos^2\alpha_1} + 2R^2V, \tag{5}$$

respectively. In Eq. (5), V is the Coulomb potential,

$$V = -\left(\frac{Z}{r_1} + \frac{Z}{r_2} + \frac{Z}{r_3}\right) + \frac{1}{r_{12}} + \frac{1}{r_{23}} + \frac{1}{r_{31}}, \tag{6}$$

where Z is the charge of the nucleus and r_{ij} is the separation between the two electrons. In this paper, we focus on the lithium atom for which $Z = 3$.

We seek to expand the wave function ψ in terms of adiabatical channel functions Φ_μ,

$$\psi = \sum_\mu F_\mu(R)\Phi_\mu(R;\Omega), \tag{7}$$

where Ω is the set of all angles ($\hat{r}_i$, α_1, and α_2) and $\Phi_\mu(R;\Omega)$ is the eigenfunction of Eq. (3) at constant hyper-radius, i.e.,

$$\frac{1}{2R^2}(T_s + W)\Phi_\mu(R;\Omega) = U_\mu(R)\Phi_\mu(R;\Omega) \tag{8}$$

with μ being a channel index. One of the major goals in the hyperspherical approach is to identify μ with a set of approximate good quantum numbers. However, this can be done only after the nature of the channel functions is understood. Note that the prefactor in Eq. (2) and $F_\mu(R)$ are totally symmetric under the permutation of any pair of electrons.

Specializing the general formula of BL to the s^3 subspace ($l_1 = l_2 = l_3 = 0$), the channel functions are given by

$$\Phi = \begin{cases} \sqrt{\frac{1}{(4\pi)^3}}\,[(P_3X)\chi_0 - (P_4X)\chi_1] & \text{if } S = 1/2 \\ \sqrt{\frac{1}{(4\pi)^3}}\,(P_2X)\chi & \text{if } S = 3/2, \end{cases} \tag{9}$$

where S is the total spin of the three electrons. Notice that for the doublet case ($S = 1/2$) the channel function consists of two intermediate spin terms constructed by coupling the first two spins into either a triplet $[\chi_1 = |(\frac{1}{2}\frac{1}{2})1, \frac{1}{2}; \frac{1}{2}\rangle]$ or a singlet $[\chi_0 = |(\frac{1}{2}\frac{1}{2})0, \frac{1}{2}; \frac{1}{2}\rangle]$ state, while a quartet spin function ($S = 3/2$) has only one term $[\chi = |(\frac{1}{2}\frac{1}{2})1, \frac{1}{2}; \frac{3}{2}\rangle]$. In Eq. (9), P_n is an element of the algebra of the S_3 group defined in BL and $X = X(R;\alpha_1,\alpha_2)$ is the radial channel function to be solved from the Schrödinger equation

$$\frac{1}{2R^2}(T_s + 2R\widetilde{W})P_nX = UP_nX, \tag{10}$$

where $n = 2$ for $S = 3/2$ and $n = 3$ (or equivalently $n = 4$) for $S = 1/2$. $2R\widetilde{W}$ is the average of W over the s^3 subspace,

$$\widetilde{W} = -Z\left[\frac{1}{\sin\alpha_1}\left(\frac{1}{\sin\alpha_2}+\frac{1}{\cos\alpha_2}\right)+\frac{1}{\cos\alpha_1}\right] + \frac{1}{\sin\alpha_1}\left(\frac{1}{\sin\alpha_2},\frac{1}{\cos\alpha_2}\right)_< + \left(\frac{1}{\sin\alpha_1\sin\alpha_2},\frac{1}{\cos\alpha_1}\right)_< + \left(\frac{1}{\sin\alpha_1\cos\alpha_2},\frac{1}{\cos\alpha_1}\right)_< \quad (11)$$

where the subscript "<" represents the smaller of the two terms in the parentheses. Notice that the repulsion between electrons is smoothed out due to averaging over the s^3 subspace. In the limits of α_1 (α_2) $\rightarrow 0$ or $\pi/2$, at least one electron is close to the nucleus and the electron-nucleus attraction is dominant, therefore $\widetilde{W}$ has steep valleys. Around the region of $r_1 = r_2 = r_3$ ($\alpha_2 = \pi/4$, $\cos\alpha_1 = 1/\sqrt{3}$), $\widetilde{W}$ is very flat. As we will see in Sec. IV, the shape of the potential $\widetilde{W}$ plays an essential role in determining the structure of channel functions as R is varied.

We solve Eq. (10) by expanding X in terms of a set of B splines [16], $B_i^1(\alpha_1)$ ($i = 1, 2, \ldots, N_1$) and $B_j^2(\alpha_2)$ ($j = 1, 2, \ldots, N_2$), of order K (=9) in the region $(0, \pi/2)$ on α_1 and α_2, respectively; the two-dimensional basis is constructed as $B_k(\alpha_1, \alpha_2) = B_i^1(\alpha_1)B_j^2(\alpha_2)$ with $k = k(i, j)$. The size of the basis is $N_s = N_1 \times N_2$. Boundary conditions at the two ends of α_1 and α_2 are imposed on the basis functions such that $B_i^1(0) = B_i^1(\pi/2) = B_i^2(0) = B_i^2(\pi/2) = 0$. Note that $P_n B_k$ ($k = 1, N_s$) is the projection of B_k onto a subspace satisfying a specified permutation symmetry. In general, the dimension of this subspace is smaller than N_s. Therefore, not all the projected functions $P_n B_k$ are independent; it is necessary to select among them the linearly independent ones.

III. ADIABATIC CHANNEL POTENTIAL CURVES

Numerical solution of Eq. (10) yields both channel functions and channel potential curves. Figures 1 and 2 display the channel potential curves $U_\mu(R)$ calculated for the quartet ($S = 3/2$) and the doublet ($S = 1/2$) states of lithium ($Z = 3$) within the s^3 subspace, respectively.

To begin with, the potential curves in the two limits, $R = 0$ and $R \rightarrow \infty$, are easily understood. At $R = 0$, Eq. (10) is dominated by T_s ("the grand angular momentum operator" [9]) whose eigenvalues are $(2J+1)(2J+2)$ with J being integers determined by the P_n symmetry. Therefore, in this region, each potential curve behaves as $(2J + 1)(2J + 2)/2R^2$. In the limit of $R \rightarrow \infty$, one electron is far away from the nucleus and the other two electrons, hence $U_\mu(R)$ must tend to one of the eigenenergies of the residual two-electron Li^+ system [10]. We checked our numerical values of channel potentials with the known eigenenergies for Li^+ and very good agreement was found. The convergence of our numerical results for large R is remarkable and illustrates the importance of solving the channel functions numerically by using the more flexible spline functions, rather than by using hyperspherical harmonics which are not suitable for large R. In fact, it was in the large-R region that the calculations of Refs. [9,10] failed.

We first look at the family of potential curves shown in Fig. 1(a) for quartet states. The potential curves at large R are easily identified. As we have mentioned, in this limit, one electron is far away from the other two and thus each potential curve approaches one of the eigenenergies of the two-electron Li^+ ion. Since the spins of these two inner electrons are parallel for quartet states, the two-electron states all have $^3S^e$ symmetry. Thus the lowest curve is labeled $1s2s$, which is a shorthand for describing the $1s2s\ ^3S^e$ state of Li^+. In accordance with the adiabatic approximation, the eigenenergies obtained by solving the one-dimensional hyper-radial equation with this lowest potential can be designated as $1s2sms\ ^4S^e$ ($m > 2$) states. This is the Rydberg series converging to the $1s2s\ ^3S^e$ excited state of Li^+. Since the Li^+ core is excited, these Rydberg states are doubly excited states. The asymptotic limit of the second lowest potential curve in Fig. 1(a) is clearly designated as $1s3s\ ^3S^e$, and the states associated with this curve are the $1s3sms\ ^4S^e$ ($m > 3$) states.

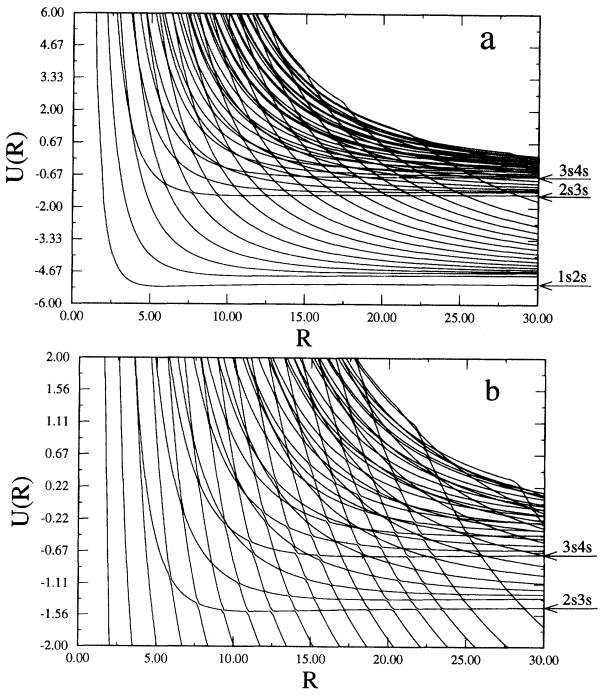

FIG. 1. The potential curves for the quartet spin state of a lithium atom as a function of R. The first members of the $1sns$, $2sns$, and $3sns$ families are labeled. The energy region where the channels support triply excited states is enlarged in (b).

By looking at potential curves in the asymptotic region, we can identify easily the group of curves which converge to singly excited states of Li^+. States associated with these curves are doubly excited states of Li. From Fig. 1(a) these curves at small R show numerous avoided crossings with another family of curves which tend to approach higher energies in the large R region. This basic structure has been observed qualitatively in the early calculations [7,9,10]. The latter group of curves converges to doubly excited states of Li^+. In Fig. 1(a) the lowest curve of this group is labeled as $2s3s\ ^3S^e$. The solutions of the one-dimensional hyper-radial equation using this potential curve can be designated as $2s3sms\ ^4S^e$ $(m > 3)$ states — they are triply excited states. In Fig. 1(b), we expand the energy region for triply excited states. The potential curves in the asymptotic region can be identified as $2s3s$, $2s4s$, ..., and then $3s4s$, $3s5s$, ..., etc. Only the "head" states of the first two groups, $2s3s$ and $3s4s$, are indicated in the figure.

We discuss next the potential curves for doublet $(S = 1/2)$ states which are shown in Fig. 2. For these states, the total spin of the two inner electrons can couple to a singlet or a triplet, thus in the asymptotic region both the singlet and triplet two-electron states exist. In Fig. 2, the lowest curve reaches the $1s^2$ limit of Li^+. The lowest eigenstate from solving the hyper-radial equation using this potential is the ground state of Li while the higher ones are singly excited states, normally designated as $1s^2ms\ ^2S^e$ $(m > 1)$. The next two higher curves in the asymptotic limit are designated as $1s2s$, the lower one is $^3S^e$ and the higher one is $^1S^e$. These two curves, and the family of curves just above them, are members of the group of curves that support doubly excited states of Li.

Figure 2 also shows another family of curves that converge to the higher energy limit in the asymptotic region. These curves support triply excited states. The lowest curve approaches the $2s^2\ ^1S^e$ state of Li^+ in the asymptotic region. Similarly the next two curves approach the $2s3s\ ^{1,3}S^e$ limits, with the triplet state being the lower one.

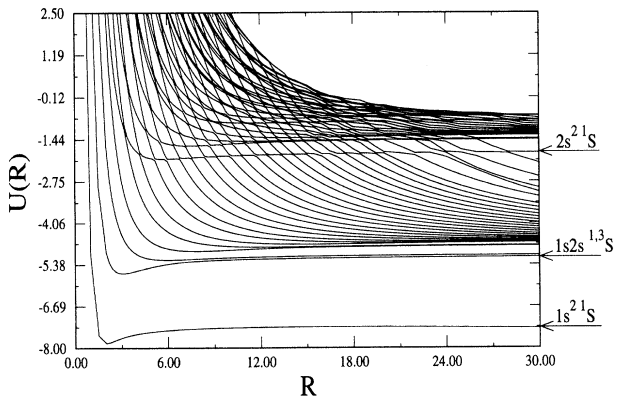

FIG. 2. The potential curves for the doublet spin state of a lithium atom as a function of R. The lowest channels which support singly, doubly, and triply excited states, respectively, are highlighted.

Therefore, within the s^3 configuration, each potential curve can be designated using the quantum numbers $Nsns$ $(n \geq N)$ that describe the two-electron states in the asymptotic region. From Figs. 1 and 2, it is clear that curves with identical N do not cross with each other. Avoided crossings can be seen among the curves with different N's which make the potential curves appear to be very complicated. These avoided crossings, on the other hand, are all very sharp. Similar to the curves in the two-electron systems, these avoided crossings will be treated as diabatic crossings in the first order approximation, thus each potential curve is a smooth function of R. As we will see in the next section, this diabatic ansatz also preserves the nodal structure of the channel function as R is varied.

IV. NODAL STRUCTURE OF CHANNEL FUNCTIONS

In order to identify approximate quantum numbers to describe the radial correlation (and angular correlation in the future) of the three-electron systems, it is desirable to display the channel wave functions. However, for the three-electron system, this is not simple. From Eq. (9) we note that the channel function for the doublet states $(S = 1/2)$ is the sum of two product terms such that the spatial wave function cannot be separated from the spin function directly. Thus the nodal structure has to be analyzed for each spin component. For the quartet states $(S = 3/2)$, the situation is simpler since the spin and the spatial part are separated. We will concentrate on the analysis of the nodal structure of channel functions for the quartet states. For the doublet states the same analysis can be applied to each spin component.

We first have to decide the domain where the channel function is to be displayed. In Fig. 3 we show the domain in terms of α_2 and $\cos\alpha_1$. The rectangle is divided into six regions, separated by three thick lines. According to our convention for the two hyperangles, the line FIB marks $r_1 = r_2$, the curve AID marks $r_2 = r_3$, and the curve HIC marks $r_1 = r_3$. Furthermore, along the four sides of the rectangle, line ABC is for r_3=0, CDE is for

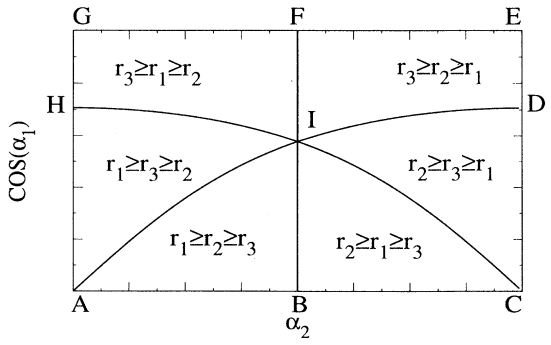

FIG. 3. The domain of $0 \leq \alpha_2 \leq \pi/2$ and $0 \leq \cos\alpha_1 \leq 1$. The line FIB marks $r_1 = r_2$, the curve AID marks $r_2 = r_3$, and the curve HIC marks $r_1 = r_3$.

r_1=0, AHG is for r_2=0, and GFE is for $r_1 = r_2$=0. The relative magnitude of the distances of the three electrons in each region is as shown.

Figure 4 displays the contour plots of the channel function of the lowest potential curve ($\mu = 1$) of Fig. 1(a) at three values of R. For quartet states, the spin part is totally symmetric, thus the spatial part is totally antisymmetric. Therefore all the quartet state wave functions should vanish along the three thick lines. These plots demonstrate that we need to consider the wave function in only one of the six regions, say ABI of Fig. 3. This is entirely expected since the three electrons are equivalent; the wave function in any one of the six regions characterizes the whole wave function. Figure 4 also shows that the nodal structure of the channel function does not change with the value of R, except that the wave function moves closer to the boundaries of the rectangle as R increases since it is the region where the potential is more negative.

We pause at this point to mention that the three thick lines in Fig. 4 set the boundaries due to the particle exchange symmetry. The fact that two of these lines are curved while one is a straight line is due to the choice of hyperspherical angles adopted in our approach. A more "democratic" choice of the coordinate system would make the boundaries simpler, but other complications such as exchange symmetry and the asymptotic limits become more complicated. This will be a subject of further study in the future.

In Fig. 5 we compare the nodal structure of the channel functions associated with the $1s2s$, $1s3s$, and $1s4s$ channels (shown only in the ABI region of Fig. 3, where $r_1 \geq r_2 \geq r_3$). If one can use the independent electron picture, the three-electron wave functions are to be designated as $1s2sms$ ($m > 2$), $1s3sms$ ($m > 3$), and $1s4sms$ ($m > 4$). In the hyperspherical approach, the nodal structure of the outermost electron is contained in the hyper-radial wave function, thus the nodal structure in the channel function reflects the nodal structure of the two inner electrons. For the $1s2s$, $1s3s$, and $1s4s$ sequence, the innermost electron is $1s$. In the domain shown in Fig. 5, this means that the wave function in r_3 is a $1s$ wave function. Since $r_3 = R\cos\alpha_1$, this means that there is no node along the horizontal direction in Fig. 5. In going from $1s2s$, $1s3s$ to $1s4s$, the second electron r_2 acquires a new node for each higher channel and this nodal line is approximately represented by $\alpha_2 = \text{const}$. Thus the channel functions for potential curves that support doubly excited states of Li acquire

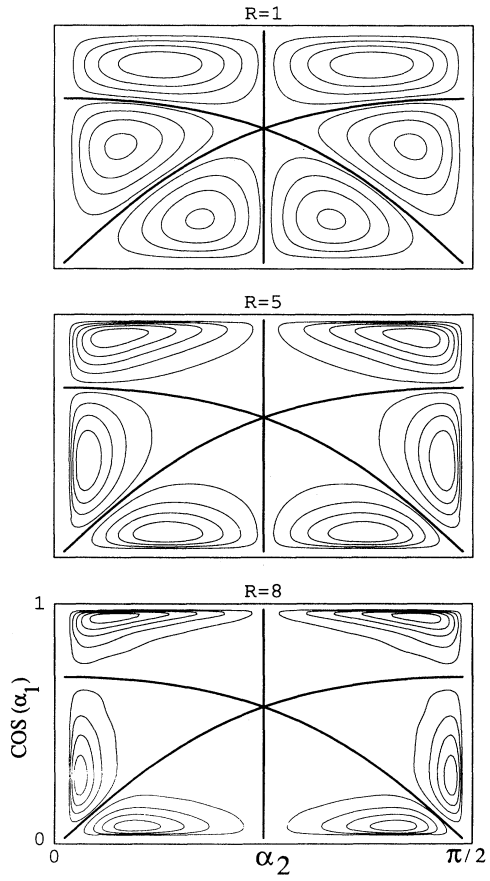

FIG. 4. The contour plot of the channel function for the lowest potential curve ($\mu = 1$) at different values of R. It is also labeled as the $1s2s$ channel. The solid lines are given by $r_1 = r_2$, $r_2 = r_3$, and $r_1 = r_3$.

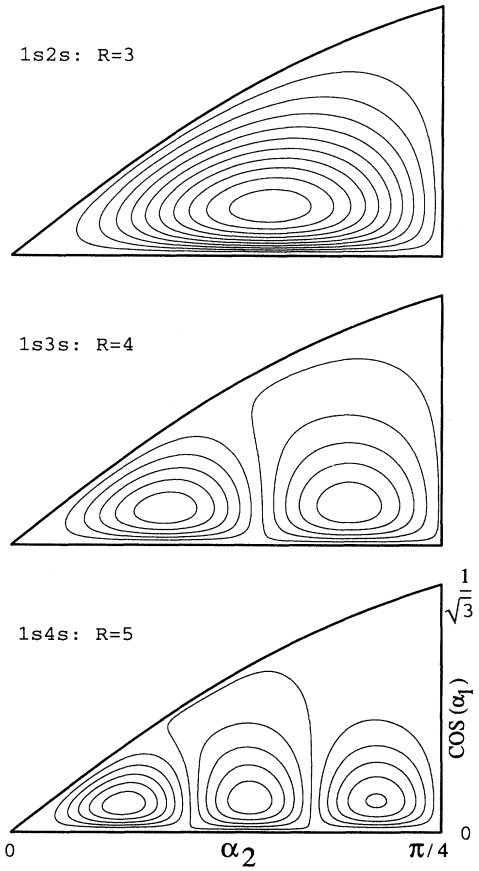

FIG. 5. The contour plots of the channel functions for the first three channels of the $1sns$ family on the domain of $r_1 \geq r_2 \geq r_3$: $1s2s$ at $R = 3$ ($\mu = 1$), $1s3s$ at $R = 4$ ($\mu = 2$), and $1s4s$ at $R = 5$ ($\mu = 3$).

more and more approximately vertical nodal lines as the second innermost electron is more excited.

We next consider the channel functions for those states which converge to doubly excited states of Li^+. The associated states are triply excited states, which according to the independent electron picture can be designated as $2s3sms$ ($m > 3$), $2s4sms$ ($m > 4$), ..., and $3s4sms$ ($m > 4$), $3s5sms$ ($m > 5$), ..., etc. The contour plot of the electron density for the lowest few of these channels is shown in Fig. 6. Since the innermost electron now also acquires nodes, horizontal nodal lines appear. Thus for $2s3s$ there is only one horizontal nodal line, and for $2s4s$ an additional vertical nodal line appears. For $3s4s$, two horizontal nodal lines appear, and for $3s5s$ an additional vertical nodal line emerges. Note we use vertical or horizontal lines only in an approximate way. We do not mean to imply that they are straight lines.

Within the approximation adopted in the present paper, we thus see how the channels are characterized in terms of the nodal structure of the channel functions.

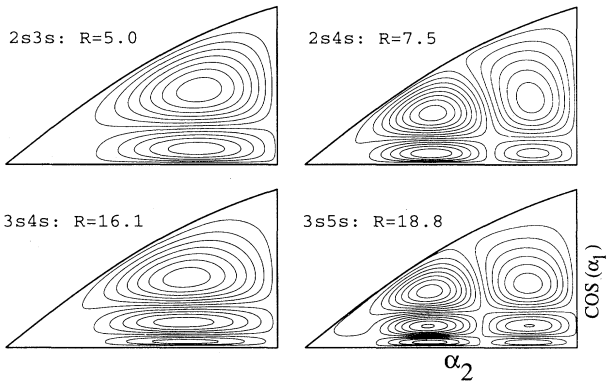

FIG. 6. The contour plots of the channel functions for the first two members of the $2sns$ family and the $3sns$ family on the domain of $r_1 \geq r_2 \geq r_3$: $2s3s$ at $R = 5$ ($\mu = 4$), $2s4s$ at $R = 7.5$ ($\mu = 7$), $3s4s$ at $R = 16.1$ ($\mu = 16$), and $3s5s$ at $R = 18.8$ ($\mu = 20$).

V. CONCLUDING REMARKS

We have studied the hyperspherical potential curves and the channel wave functions of Li within the subspace of $l_1 = l_2 = l_3 = 0$. The properties of both channel potential curves and channel functions show that they can be classified by the nodal lines in the two hyperangles which in turn can be explained approximately by the independent particle quantum numbers. These quantum numbers group the channel potential curves into different families and the sharp avoided crossings between curves of different families can be treated diabatically. Further calculations including mixing of different (l_1, l_2, l_3) subspaces are underway, which indicates that the group structure among the channel potential curves remains and the results will be discussed elsewhere.

ACKNOWLEDGMENTS

One of us (X.Y.) wishes to thank Dr. Joachim Burgdörfer, Dr. Chris Greene, and Yan Zhou for simulating discussions. This work is supported in part by the U.S. Department of Energy, Office of Energy Research, Office of Basic Energy Sciences, Division of Chemical Sciences.

[1] R. P. Madden and K. Codling, Phys. Rev. Lett. **10**, 516 (1963).
[2] See C. D. Lin, in *Review of Fundamental Processes and Applications of Atoms and Ions*, edited by C. D. Lin (World Scientific, Singapore, 1993), p. 357, and the literature cited therein.
[3] J. H. Macek, J. Phys. B **2**, 831 (1968); C. D. Lin, Phys. Rev. A **10**, 1986 (1974); U. Fano and C. D. Lin, *Atomic Physics* (Plenum, New York, 1975), Vol. 4, p. 47. For a recent review, see C. D. Lin, Phys. Rep. (to be published).
[4] D. R. Herrick and O. Sinanoglu, Phys. Rev. A **11**, 97 (1975).
[5] C. D. Lin, Phys. Rev. A **29**, 1019 (1984).
[6] J. Z. Tang, S. Watanabe, and M. Matsuzawa, Phys. Rev. A **46**, 2437 (1992); B. Zhou, C. D. Lin, J. Z. Tang, S. Watanabe, and M. Matsuzawa, J. Phys. B **26**, 2555 (1993).
[7] S. Watanabe, M. Le Dourneuf, and L. Pelamourgues, J. Phys. Suppl. **43**, C2-223 (1982).
[8] Ruiqin Zhang and Conghao Deng, Phys. Rev. A **47**, 71 (1993), and references therein.
[9] C. W. Clark and C. H. Greene, Phys. Rev. A **21**, 1786 (1980).
[10] C. H. Greene and C. W. Clark, Phys. Rev. A **30**, 2161 (1984).
[11] U. Fano and A. R. P. Rau, *Atomic Collisions and Spectra* (Academic Press, Orlando, 1986).
[12] C. G. Bao and C. D. Lin, Few-Body Systems **16**, 47 (1994).
[13] K. H. Al-Bayati and K. E. Banyard, J. Phys. B **20**, 465 (1987); S. Watanabe and C. D. Lin, Phys. Rev. A **36**, 511 (1987); Y. Komninos, M. Chrysos, and C. A. Nicolaides, *ibid.* **38**, 3182 (1988); K. T. Chung, *ibid.* **44**, 5421 (1991); **45**, 7766 (1992); **46**, 6914 (1992); C. A. Nicolaides, N. A. Piangos, and Y. Komninos, *ibid.* **48**, 3578 (1993); C. G. Bao, W. F. Xie, and C. D. Lin, J. Phys. B **27**, L193 (1994).
[14] L. M. Kiernan, E. T. Kennedy, J-P. Mosnier, and J. T. Costello, Phys. Rev. Lett. **72**, 2359 (1994).
[15] Y. Azuma, *et al.*, Phys. Rev. Lett. (to be published).
[16] J. Xi, X. He, and B. Li, Phys. Rev. A **46**, 5806 (1992), and the literature cited therein.